Thermal stability of high density polyethylene–fumed silica nanocomposites

A. Dorigato · A. Pegoretti · A. Frache

Abstract High-density polyethylene-based nanocomposites were prepared through a melt compounding process by using surface functionalized fumed silica nanoparticles in various amounts, in order to investigate their capability to improve both mechanical properties and resistance to thermal degradation. The fine dispersion of silica aggregates led to noticeable improvements of both the elastic modulus and of the stress at yield proportionally to the filler content, while the tensile properties at break were not impaired even at elevated filler content. Thermogravimetric analysis showed that the selected nanoparticles were extremely effective both in increasing the decomposition temperature and in decreasing the mass loss rate, even at relatively low filler loadings. The formation of a char enriched layer, limiting the diffusion of the oxygen through the nanofilled samples, was responsible of noticeable improvements of the limiting oxygen index, especially at elevated silica loadings. In contrast with commonly reported literature results, cone calorimeter tests also revealed the efficacy of functionalized nanoparticles in delaying the time to ignition and in decreasing the heat release rate values. Therefore, the addition of functionalized fumed silica nanoparticles could represent an effective way to enhance the flammability properties of polyolefin matrices even at low filler concentrations.

A. Dorigato (✉) · A. Pegoretti
Department of Materials Engineering and Industrial Technologies (DIMTI), University of Trento, via Mesiano 77, 38123 Trento, Italy
e-mail: andrea.dorigato@ing.unitn.it

A. Frache
Department of Materials Science and Chemical Engineering (DISMIC), Polytechnic of Turin, Via T. Michel 5, 15100 Alessandria, Italy

Introduction

A deep interest has emerged in the use of nanostructured materials as fillers to improve the properties of polymeric matrices [1, 2]. In fact, the addition of small amounts of nanofiller (up to 5–10 wt%) to polymers may improve their mechanical behaviour (stiffness [3–6], failure resistance [7, 8] and dimensional stability [6, 9, 10]), their gas and solvents barrier properties [11–13] and their thermal degradation and chemical resistance [6, 13, 14], avoiding the drawbacks (embrittlement, loss of transparency and loss of lightness) usually associated to the addition of traditional microfillers [15, 16].

High-density polyethylene (HDPE) is one of the most widely used thermoplastic polymers, but for some technological applications its relatively poor stiffness and creep resistance, accompanied by a relatively low thermal stability, may represent a severe limitation [17, 18], and crosslinking is often unavoidable. The introduction of relatively small amounts of nanoparticles has been proven to be a viable method to solve these problems [19]. The problem of the nanofiller dispersion within the matrix has been tackled by organomodification of the clay nanoplatelets [6, 20–22]. Furthermore, addition of polyethylene grafted with maleic anhydride has been proven to favour the intercalation/exfoliation process, with remarkable enhancements of the material performances [9, 23, 24].

For as concerns the thermal stability, noticeable improvements were obtained through the introduction of organoclays in HDPE. For instance, Lu et al. investigated the morphology and flammability properties of γ-ray

crosslinked maleated polyethylene/clay nanocomposites Cone calorimetry tests showed that the improvement in heat release rate (HRR) for irradiated materials was suppressed by the nanodispersion of clay layers, especially at high irradiation dose levels [23]. Other polyethylene-based nanocomposites containing organically modified hydrotalcites were studied by Costantino et al. [25, 26] with interesting results in terms of both thermo-oxidative stability and improvements in the combustion behaviour. It is generally believed that the improvement of flammability properties induced by layered silicates is due to the formation of a clay-enriched protective char during combustion [27, 28].

Quite surprisingly, less attention have been devoted to polyethylene-based nanocomposites filled with isodimensional nanofillers, such as fumed silica nanoparticles. Due to its fractal structure and its high specific area, fumed silica is prone to self-aggregation and can consequently form a network of connected or interacting particles in polymer matrices [29]. It has been recently demonstrated that the mechanical performances of various thermoplastic matrices can be substantially improved by the introduction of this kind of nanoparticles [29–34]. For instance, Barus et al. [35] prepared HDPE nanocomposites by dispersing nanosilica particles with and without surface modifiers. Depending on the kind of surfactant employed, thermogravimetric (TG) analysis showed stabilization phenomena similar to that reported in literature for nanocomposites based on clays, especially in oxidant atmosphere. Chrissafis et al. [36, 37] investigated the thermal degradation mechanism of HDPE-based nanocomposites, containing various amounts of untreated fumed silica nanoparticles. Even in this case the fine dispersion of the nanoparticles at the nanoscale produced an important enhancement of the thermal stability, as evidenced by TG tests under non-isothermal conditions.

In many articles dealing with flame retardancy of polymer nanocomposites, the stabilizing effect provided by the nanofillers was assessed only by TG measurements, without considering that the thermal behaviour of nanocomposites is the result of several mechanisms that are strongly dependent from the actual fire scenario. As explained in the comprehensive review of Kiliaris et al. [28] on the flame retardancy of polyethylene/clay nanocomposites, the generation of a superficial carbonaceous-silicate charred layer is responsible of the observed reduction of the peak heat release rate (pHRR) in cone calorimetry tests, but does not influence the time to ignition (TTI) or the total heat released (THR). Furthermore, nanocomposites generally do not perform equivalently well in other important flammability analyses, such as the *UL94V* burning test and the limiting oxygen index (LOI) test. In these tests, barrier formation plays a limited effect,

while the change in viscosity and thus dripping characteristics is the governing parameter.

Recently, we have investigated the role of the filler surface properties on the thermal and mechanical properties of HDPE–fumed silica nanocomposites [38]. In that article, a high-density polyethylene matrix was melt compounded with various untreated (hydrophilic) or surface-treated (hydrophobic) fumed silica nanoparticles, having different surface areas. It emerged that surface treated nanoparticles (i.e. Aerosil® r974) were the most efficient in improving both thermo-oxidative resistance and mechanical properties. Therefore, in this article thermal stability of nanocomposites containing various amounts of Aerosil® r974 (from 1 to 8 vol%) was studied. The microstructural features of the samples were investigated through electron microscopy and correlated to their mechanical performances and dimensional stability, while the thermal degradation behaviour was characterized by various techniques, such as TG analysis, LOI determination and cone calorimetry tests.

Experimental

Materials

An Eltex A 4009 MFN1325 HDPE, having density of 0.96 g cm^{-3}, melting temperature of 136 °C, melt flow rate (MFR) at 190 °C and 2.16 kg of 0.9 g (10 min)$^{-1}$, was supplied by Ineos Polyolefins (Grangemouth, UK) as fine powder. On the basis of our previous study on the thermo-mechanical characterization of HDPE–fumed silica nanocomposites [38], Aerosil® r974 fumed silica nanoparticles, supplied by Degussa (Hanau, Germany), were utilized. This is a particulate nanofiller constituted by aggregates of equiaxic primary nanoparticles having a mean size of 12 nm (SiO$_2$ content 99.8 %). These nanoparticles are characterized by a surface area of 170 m^2 g^{-1} and were surface treated with dimethyldichlorosilane, for a total carbon content between 0.7 and 1.3 wt%, and a pH value in 4 wt% aqueous solution of 3.7–4.7. This nanopowder is characterized by a bulk density of 1.99 g cm^{-3} and a tamped density of 60 g l^{-1}. Both matrix and nanoparticles were utilized as received.

Sample preparation

Polyethylene–silica nanocomposites were prepared by a melt compounding process, using a Haake PolyLab system (Karlsruhe, Germany) consisting of a Rheomix 600 internal mixer and a Rheocord 300p control module for continuous monitoring of torque, motor speed and temperature. Both neat HDPE and relative nanocomposites with different

silica amounts (2, 4 and 8 vol%) were melt-mixed for 10 min at a temperature of 155 °C and a rotor speed of 60 rpm. Square sheet samples with different thickness (0.8 and 4 mm) were then obtained by compression moulding for 10 min at 155 °C in a Carver laboratory press (Wabash, IN, USA) under an applied pressure of 0.2 kPa. Both polyethylene powder and fumed silica nanoparticles were utilized as received. For shortness, unfilled HDPE was denoted as PE, while nanocomposites were designated as PE followed by the silica type (Ar974) and the filler content. As an example, PE-Ar974-2 indicates the nanocomposite sample filled with the 2 vol% of Aerosil r974 fumed silica nanoparticles.

Experimental methodologies

In order to evaluate the influence of the dispersion state of the selected nanoparticles in the PE matrix, field emission scanning electron microscope (FESEM) images of prepared nanocomposites were taken through a Zeiss (Cambridge, UK) Supra 40 microscope, operating at an acceleration voltage of 10 kV. The samples were cryo-fractured in liquid nitrogen and observed after a metallization process.

Uniaxial tensile tests were performed at room temperature by using an Instron$^\circledR$ 4502 (Norwood, MA, USA) tensile testing machine on ISO 527 1BA dogbone specimens, 5-mm wide and 0.8-mm thick. Elastic modulus was evaluated at a crosshead speed of 0.25 mm min^{-1}, and the strain was recorded through an Instron 2620-601 (Norwood, MA, USA) resistance extensometer, having a gage length of 12.5 mm. According to ISO 527 standard, the elastic modulus was determined as a secant value between deformation levels of 0.05 and 0.25 %. Tensile tests at break were conducted at a crosshead speed of 50 mm min^{-1} without using the extensometer, and the deformation was monitored normalizing the crosshead displacement over the gage length of the samples (30 mm). In this way the tensile properties at yield (σ_y) and at break (σ_b, ε_b) were determined. At least five specimens were tested for each sample.

Vicat softening temperature was determined by an ATS-FAAR mod. MP/3 apparatus (Milan, Italy) according to ASTM D1525 standard. Rectangular samples 10-mm long, 5-mm wide and 4-mm thick were tested, imposing a load of 10 N and a temperature ramp from 30 to 200 °C at 50 °C min^{-1}. At least three specimens were tested for each sample. TG analyses were conducted by a Mettler TG50 thermobalance (Schwerzenbach, Switzerland) in a temperature range from 30 to 700 °C at a heating rate of 10 °C min^{-1} under a constant air flow of 100 ml min^{-1} on specimens of about 50 mg. In this way it was possible to evaluate the temperatures associated to a mass loss of 2, 5

and 20 %, respectively, denoted as $T_{2\%}$, $T_{5\%}$ and $T_{20\%}$, the maximum degradation rate temperature (T_d) and the maximum mass loss rate (MMLR). The determination of the LOI was performed using a CEAST apparatus (Turin, Italy) according to ASTM D2683 standard. Rectangular samples, 80-mm long, 10-mm wide and 4-mm thick were utilized. At least 15 specimens were tested for each sample. The dependency of the flame propagation rate from the oxygen concentration was also evaluated. A Fire Testing Technology cone calorimeter (East Grinstead, UK) was used under a heat flux of 35 kW m^{-2} according to ISO 5660-1 to evaluate the combustion behaviour of the materials. The parameters measured were TTI (s), THR (kW m^{-2}), HRR (kW m^{-2}), the relative peak (pHRR, kW m^{-2}) and the total smoke release (TSR, m^2 m^{-2}). Three specimens (100 × 100 × 4 mm^3) were tested for each formulation.

Results and discussion

Morphological characterization

The microstructure of cryo-fractured nanocomposite samples can be observed in FESEM images reported in Fig. 1a–c. It is evident that fumed silica nanoparticles are uniformly dispersed in the matrix at all the investigated filler concentrations, forming isodimensional clusters of aggregated primary nanoparticles having a mean size <200 nm. As reported by Chrissafis et al. [36, 37], this aggregated morphology is characteristic of fumed silica, and can be attributed to the strong interaction between the surface hydroxyl groups of the nanoparticles [39, 40]. It is often reported that surface treatment of inorganic fillers with organic surfactants or coupling agents could lead to a decrease of their surface free energy and thus of their wettability [41]. For instance, maleinated molecules adsorb strongly on the surface of the filler, while organosilanes can form a polysiloxane layer on it [42]. In these conditions, interparticle interactions are reduced and the nanofiller dispersion within the matrix could be improved. Although filler dispersion state in polymer nanocomposites is often investigated by electron microscopy (SEM, TEM), dynamic rheological measurements could be more effective and less subjective in detecting filler networking within the matrix [43, 44]. In fact, the formation of the network considerably modifies the rheological properties of nanocomposite melts, and a yield stress appears at low shear rates [29]. A detailed description about the dynamic rheological behaviour of these composites will be reported in a future communication.

It is worthwhile to note that the mean size of the aggregates is proportional to the filler content. PE-Ar974-2

Fig. 1 FESEM images of neat PE and relative nanocomposites, magnification = ×50,000. a PE-Ar974-2, b PE-Ar974-4 and c PE-Ar974-8
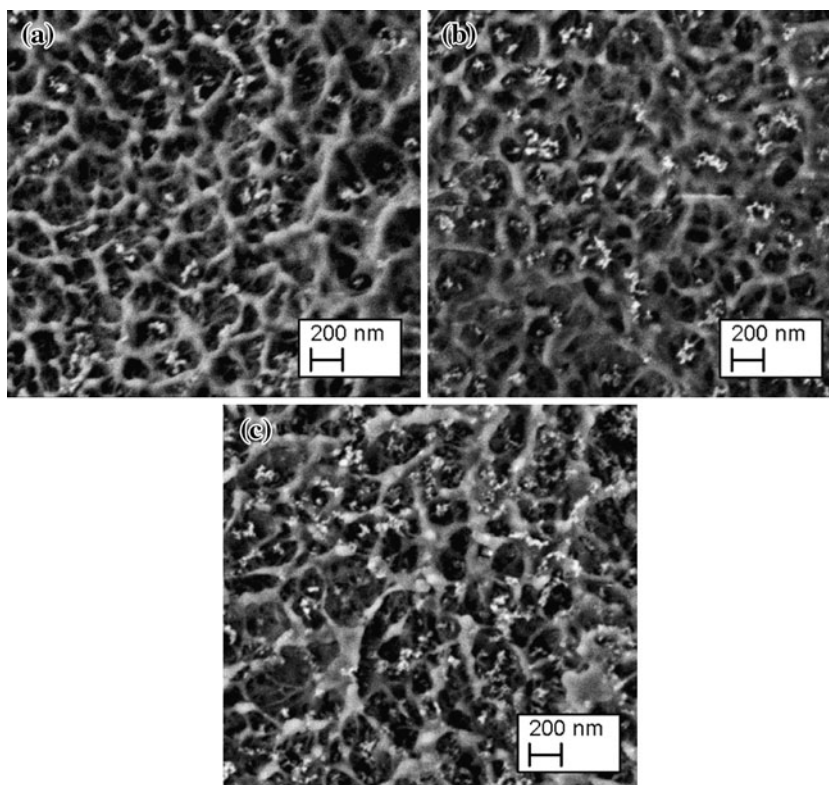
samples is characterized by the presence of aggregates having a mean diameter of 80 nm, while the mean dimension of silica aggregates for 4 and 8 vol% nanocomposites is slightly higher (110 and 150 nm, respectively). As mentioned in our previous article [38], increasing the filler amount the mean distance between silica aggregates diminishes and the probability of nanofiller aggregation is therefore enhanced.

Mechanical properties

The presence of an aggregated microstructure is also reflected into the mechanical properties of the prepared samples. In Fig. 2, representative stress–strain curves of pure PE and relative nanocomposites from quasi-static tensile tests are reported, while in Table 1 the most important mechanical properties are summarized. It can be noticed that elastic modulus (E) increases continuously by increasing silica content. For PE-Ar974-8 nanocomposite a remarkable 46 % increase of the elastic modulus can be observed with respect to the neat matrix. Also the tensile stress at yield (σ_y) is sensibly increased by nanofiller addition. Both stress and strain at break increase up to a silica content of 2 vol%, and then decrease, probably because of the formation of larger aggregates (see FESEM micrographs in Fig. 1). It is likely that the good dispersion of fumed silica aggregates at the nanoscale level leads to relatively lower stress concentration and cracking
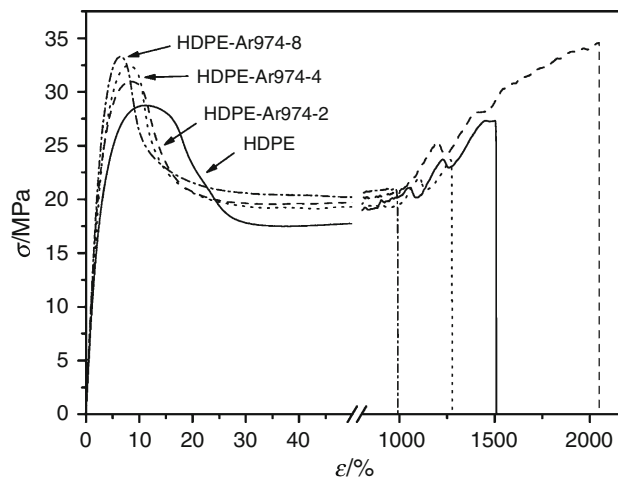
Fig. 2 Representative stress–strain curves of neat PE and relative nanocomposites from uniaxial tensile tests at break

nucleation phenomena at the interface. The formation of silica aggregates having a mean size >100 nm seems to produce a slight embrittlement of the samples. The drop of the tensile properties at break for the nanocomposites at high filler contents is a well-known phenomenon [1, 2, 45]. However, the embrittlement observed on these materials is not dramatic, probably because the mean diameter of the aggregates is <200 nm even at a filler content of 8 vol%.

In order to investigate the retention of mechanical stability as temperature increases, Vicat softening temperature

Table 1 Quasi-static tensile properties and Vicat grade of neat PE and relative nanocomposites

Sample	E/GPa	σ_y/MPa	σ_b/MPa	ε_b/%	VST/°C
PE	1.19 ± 0.02	29.6 ± 0.5	24.3 ± 1.4	1,381 ± 231	132.4 ± 1.1
PE-Ar974-2	1.24 ± 0.04	31.0 ± 0.6	34.4 ± 0.5	2,035 ± 172	133.0 ± 0.4
PE-Ar974-4	1.64 ± 0.04	32.6 ± 0.4	23.1 ± 0.3	1,237 ± 46	133.4 ± 0.6
PE-Ar974-8	1.74 ± 0.02	33.7 ± 0.4	20.6 ± 0.2	912 ± 149	133.5 ± 0.3

(VST) was evaluated. Penetration profiles of the investigated nanocomposites recorded during Vicat tests are reported in Fig. 3, while in Table 1 the Vicat temperatures, corresponding to a 1-mm penetration depth, are summarized. It can be observed that the temperature at which the penetration of the probe begins is sensibly shifted towards higher temperatures as the nanofiller amount increases. However, it is also evident that the penetration rapidly increases only at temperatures approaching the melting point of the HDPE matrix. Consequently, only slight enhancements of the Vicat grade can be detected for nanofilled samples (only 1 °C for a filler content of 8 vol%). This behaviour can be explained considering that VST of a semicrystalline polymer is generally lower than its melting temperature, because of a decrease in the modulus with temperature [46]. Reinforcement with inorganic fillers can increase the modulus of the composite, thus increasing the VST significantly to near the melting point. It is evident that when a high crystalline polymer is considered (such as HDPE), the VST of the neat matrix is near the melting temperature, because only a small fraction of the material (the amorphous part) can relax above the glass transition temperature (T_g). Consequently, only a small contribution on the VST can be seen for this kind of matrices. To support our experimental evidences, it could be noticed that also Gungor [47], studying the effect of iron

microparticles on the physical and mechanical properties of high-density polyethylene composites, found that the VST was increased by only 3 °C at a filler content of 10 vol%. For as concern nanofilled polymers, in literature it can be generally found that the introduction of nanoparticles may increase the Vicat grade with respect to the neat matrix. In an article of Pan et al. [48], Vicat softening temperature tests were performed on PVC/clay nanocomposites at different clay loadings. It was found that the VST of nanocomposites exhibited a progressively increasing trend with increasing clay content (+15 °C with a filler amount of 6 wt%). In this case, the enhancement of the VST temperature was attributed to the increased thermal insulation effect of clay nanoplatelets. Less intense enhancements in the VST were detected by Shen et al. on PA6-silica nanocomposites (+9 °C for a filler concentration of 10 wt%). Even for nanofilled samples, the experienced increase of the Vicat grade due to nanofiller introduction is reduced when a relatively high crystalline matrix was considered, as reported in the study of Bikiaris et al. [49], in which the VST of an isotactic polypropylene matrix (degree of crystallinity of 63 %) was increased by only 5 °C for a fumed silica content of 15 wt%.

Thermal properties

Results of TG analysis on neat HDPE and relative nanocomposites are reported in Fig. 4. In particular, Fig. 4a compares mass loss as a function of temperature, while in Fig. 4b derivative of the mass loss curves are plotted. The HDPE matrix in contact with air at about 250–300 °C subjected to reactions of oxygen insertion, forming peroxy radical species [50]. The subsequent formation of other oxidized species promotes chain scission. Above 350 °C polyethylene suffers a strong mass loss to form a 5 wt% residue at 470 °C, which is completely oxidized to volatile products at 550 °C. Neat PE samples decompose in a two-step process. The first mass loss is located in a temperature range from 350 to 410 °C (about 50 % mass loss takes place in this region), while the second is in the temperature range from 410 to 480 °C (mass loss of 45 %). In the differential TG plots of Fig. 4b, these two steps correspond to sharp decomposition maxima located at about 390 and 460 °C, respectively. The presence of silica nanoparticles
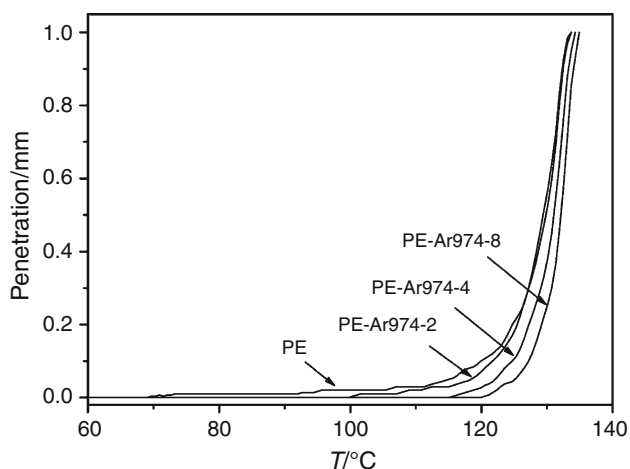
Fig. 3 Penetration profiles of neat PE and relative nanocomposites in the tests for the determination of the Vicat grade
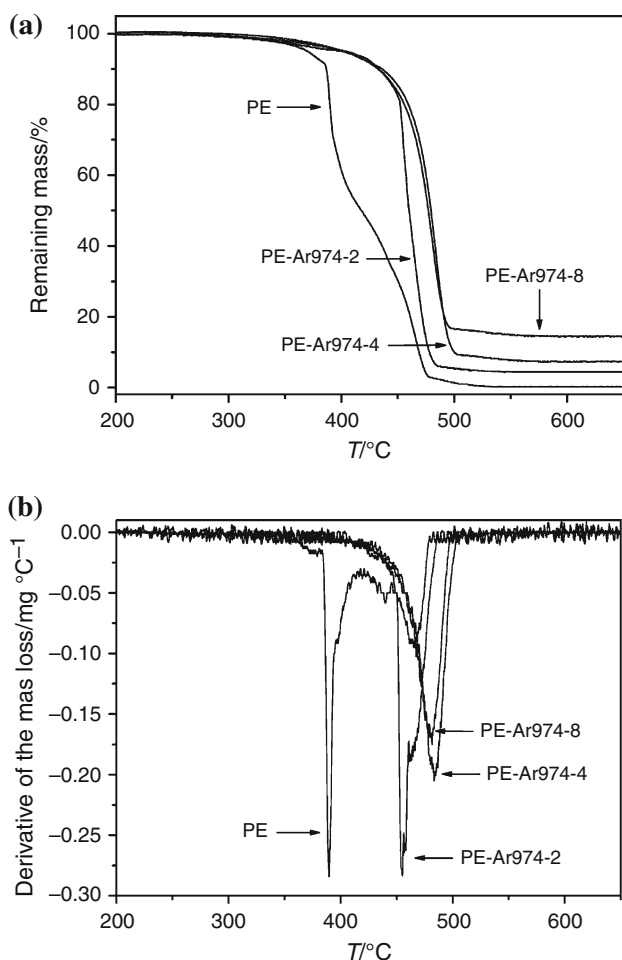
Fig. 4 TG tests of neat PE and relative nanocomposites under oxygen atmosphere. **a** Remaining mass and **b** derivative of the mass loss as a function of temperature

Table 2 Results of TG measurements on neat PE and relative nanocomposites

Sample	$T_{2\%}^{a}$/°C	$T_{5\%}^{b}$/°C	$T_{20\%}^{c}$/°C	T_{d}^{d}/°C	MMLR/ mg °C^{-1}
PE	335.3	370.7	390.0	389.7	0.284
PE-Ar974-2	360.0	403.7	452.0	455.0	0.283
PE-Ar974-4	347.7	401.0	458.0	483.3	0.205
PE-Ar974-8	336.7	400.7	455.7	481.7	0.175

MMLR maximum mass loss rate

[a] Temperature corresponding to 2 % mass loss

[b] Temperature corresponding to 5 % mass loss

[c] Temperature corresponding to 20 % mass loss

[d] Degradation temperature (maximum of the mass loss rate)

noticeably changes the thermal decomposition behaviour with respect to the neat matrix. The low temperature decomposition peak is completely suppressed and most part of the material decomposes at temperatures above 450 °C. An increase of nanosilica concentration up to 4 vol% produces a shift of the MMLR temperature up to 480 °C, with an interesting decrease of the mass loss rate. A further increase of the filler content up to 8 vol% induces a reduction of the mass loss rate, while the peak temperature remains practically the same. The residue left after combustion of neat PE in air is nearly zero, as all the organic components decompose into gaseous products, while the remaining mass at 700 °C of the nanofilled samples corresponds to the actual nanosilica mass percentage (very close to the theoretical one). The positive effect of fumed silica on the thermal degradation resistance of the nanocomposites is clearly manifested in an increase of $T_{2\%}$, $T_{5\%}$ and $T_{20\%}$ values reported in Table 2, which represent the temperatures corresponding to a mass loss of

2, 5 and 20 wt%, respectively. In particular, $T_{5\%}$, that is often considered as the onset degradation temperature, increases by about 30 °C, while even more important enhancements can be registered for $T_{20\%}$ (up to 65 °C). It is interesting to note that $T_{2\%}$ decreases at high filler content up to values similar to that of neat PE. As already reported by other authors [51, 52], this drop can be explained by the relatively high amount of thermally less stable organic species introduced through surface-treated silica. According to the general theories on the flame resistance of polymer nanocomposites [6, 14], the stabilization phenomena observed for nanosilica filled samples could be explained in terms of their ablative behaviour. In fact, during the thermal degradation of the specimen, silica aggregates probably tend to agglomerate on the surface of the molten polymer, thus creating a barrier that physically protects the rest of the polymer and hinders the volatilization of the oligomers generated during the combustion process. This consideration could also explain the absence of the first degradation step at 390 °C for the nanofilled samples (Fig. 4a). It is clear that the ability to form this protective shield will depend on the capability of silica aggregates to form a continuous barrier. According to FESEM images reported in Fig. 1, the relatively fine dispersion of silica aggregates at all the considered concentrations permits the creation of an efficient barrier even at low filler contents. Increasing the silica amount, the mean distance between the aggregates is considerably reduced, and the formation of a thicker and stronger protective shield is therefore favoured.

Flammability test

In order to collect more experimental information on the real effectiveness of silica nanoparticles as fire retardant additives, LOI values of neat PE and relative nanocomposites were determined. Figure 5 shows a linear dependency of the flame propagation rate on the oxygen

concentration, both for neat PE and for nanofilled samples. It can be clearly observed that the introduction of fumed silica nanoparticles is responsible of a strong shift towards higher oxygen concentrations, proportionally to the filler content. Furthermore, the propagation rate sensitivity to the oxygen concentration, expressed by the slope of the lines in Fig. 5, is considerably reduced by nanosilica introduction. Consequently, as summarized in Table 3, LOI values of the nanofilled samples are considerably enhanced. The unfilled HDPE presents a LOI value of 20.4, which is slightly higher with respect to the values commonly reported in literature for an inflammable matrix such as polyethylene (generally around 18). In any case, it is not uncommon to find literature articles in which values of LOI higher than 19 are reported [53, 54]. What is important to underline is that the addition of even a low amount of nanosilica induces a noticeable improvement of the LOI value up to 25.9. An increase of the silica amounts up to 8 vol% leads to an increase of the LOI up to 28.1 (+38 % compared to unfilled matrix). It can be useful to remind that, according to the general classification of the fire properties of plastics, a polymer matrix having a LOI higher than 22.5 is considered flame retardant, while above 27.0 the material is self-extinguishing [55].
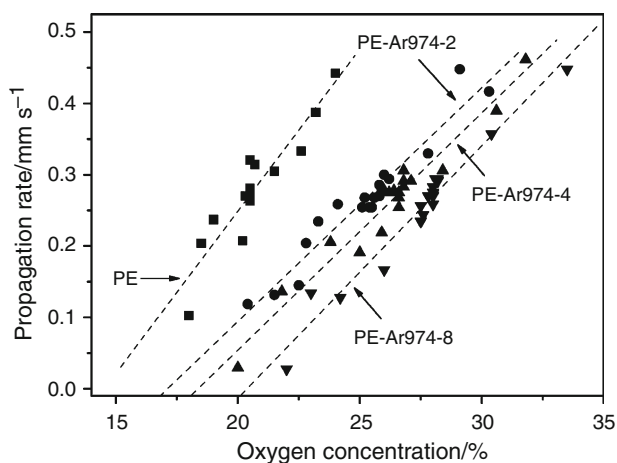
Fig. 5 Dependency of the flame propagation rate from the oxygen concentration in the tests for the determination of the LOI values. *Filled square* PE, *filled circle* PE-Ar974-2, *filled triangle* PE-Ar974-4, *filled inverted triangle* PE-Ar974-8

Table 3 LOI values of neat PE and relative nanocomposites

Sample	LOI/%
PE	20.4
PE-Ar974-2	25.9
PE-Ar974-4	26.7
PE-Ar974-8	28.1

It can be also important to analyze how the materials burn at oxygen concentrations near the LOI value. Therefore, representative images of the flame propagation stages acquired during LOI tests on neat PE and on PE-Ar974-8 nanocomposite at two different oxygen concentrations (21 and 28 %) are collected in Figs. 6 and 7, respectively. A parabolic propagation field is formed during the combustion of the samples, this means that the flame propagation starts from the surface layer and then gradually reaches the core. In the unfilled polyethylene, the molten polymer (Fig. 6a) burns rapidly with evident dripping until the whole consumption of the sample is reached (Fig. 6f). In case of nanofilled samples, the surface layer is immediately covered by a residue of char (Fig. 7a–c). The molten polymer covered by this protective layer remains supported on the solid unburned region (Fig. 7d–e), and at the end of the tests it collapses under its own weight (Fig. 7f). No dripping was observed during the tests on the nanofilled samples, even at lower silica amounts. This
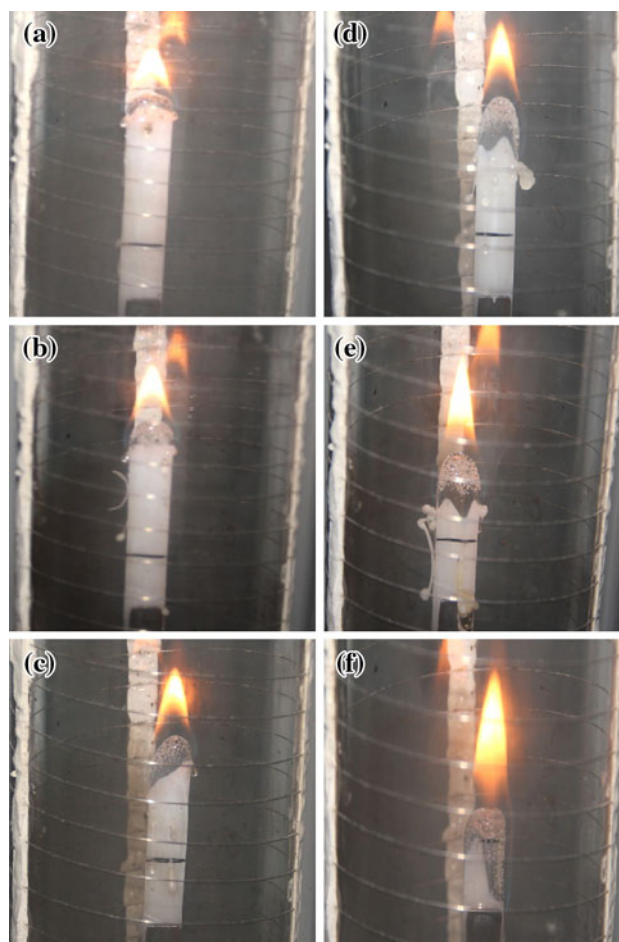
Fig. 6 Representative images of the flame propagation stages in the tests for the determination of the LOI values of neat PE (oxygen concentration = 21 %). **a** 20 s, **b** 40 s, **c** 60 s, **d** 120 s, **e** 160 s and **f** 200 s
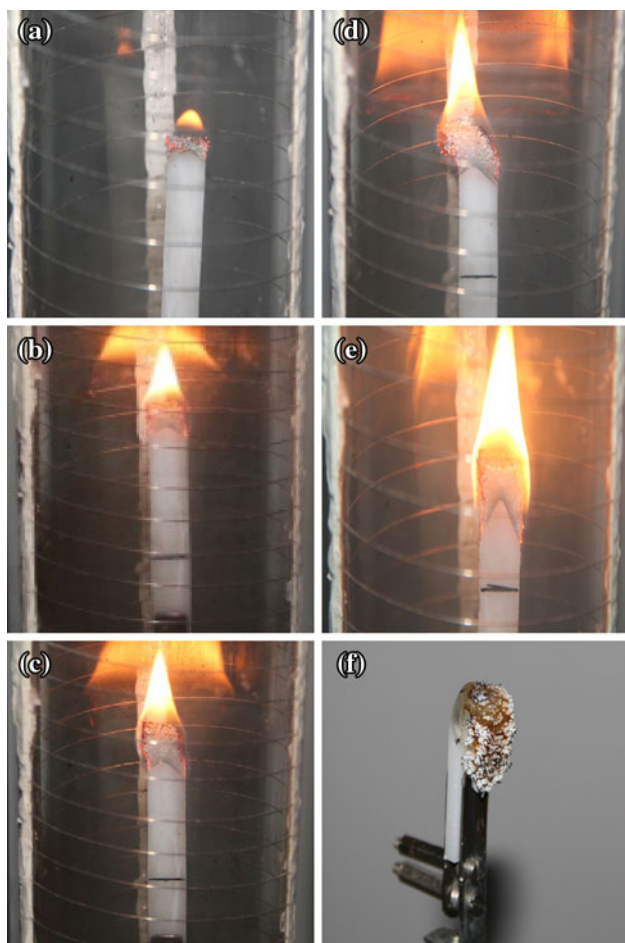
Fig. 7 Representative images of the flame propagation stages in the tests for the determination of the LOI values of PE-Ar974-8 nanocomposite (oxygen concentration = 28 %). **a** 20 s, **b** 40 s, **c** 60 s, **d** 120 s, **e** 140 s and **f** burned sample

evidence could be explained considering the noticeable increase of the melt viscosity induced by the presence of the nanofiller [29, 56]. For sustaining the burning process in the nanofilled samples, it is also clear that the heat must be conducted from the flame-front into the melt region passing through the char layer. Thus, the char layer acts as a physical barrier against the propagation of the flame. At low silica contents, the thickness of char layer formed on the burning surface is very small, and its effectiveness as physical barrier is therefore rather limited. Increasing nanofiller amount, the thickness of the protective layer increases, making the self-sustained burning of the sample more and more difficult at low oxygen concentrations and thus increasing the LOI value. In our case, an important increase of the LOI values and the total absence of the dripping of the molten polymer are obtained even at relatively limited silica amounts (2 vol%), evidencing the strong effectiveness of surface-treated fumed silica nanoparticles as fire retardant additives. The increase of the melt

viscosity induced by the nanoparticles not only prevents melt dripping, but also plays an important role in determining LOI values of the nanofilled samples. In fact, if the viscosity of the melt is not sufficient to hold the residue vertically placed on the specimen, it drips down continuously, exposing fresh surfaces to flame and promoting continuous burning of the specimen. Introducing an appropriate amount of nanosilica, the high melt viscosity prevents its flowing and holds the char layer on the sample stock, making difficult a further flame propagation and increasing LOI values. Even if in literature it is often reported that nanocomposites do not perform better than pristine polymers in LOI test without the introduction of small amounts of flame retardants [28], in some cases interesting improvements of LOI values were obtained for polyethylene-based nanocomposites. For instance, Costa et al. [50] utilized layered double hydroxides (LDHs) to prepared LDPE nanocomposites by melt compounding, reporting an increment of the LOI value of 22 % over that of the neat matrix with a filler content of 20 wt%. Minkova et al. [54] investigated the thermal stability of compatibilized high-density polyethylene/clay nanocomposites, finding that LOI values of 3 wt% filled nanocomposites were 15 % higher than that of the pristine matrix. In our case the LOI value of PE-Ar974-2 sample (silica content of 4 wt%) is 27 % higher than that of the neat PE. These comparisons confirm the effectiveness of the selected nanoparticles in improving the flammability properties of the polyethylene matrix.

Combustion behaviour

The use of the cone calorimetry to complete the characterization of these nanocomposites can provide helpful information about the combustion of the polymers
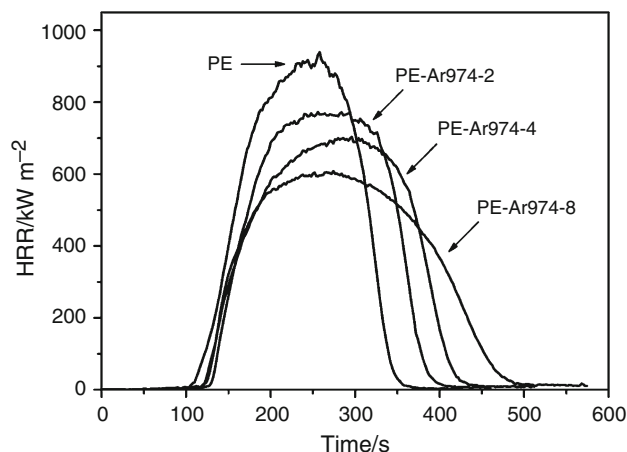
Fig. 8 HRR curves of neat PE and relative nanocomposites

Table 4 Combustion data of neat PE and relative nanocomposites from cone calorimeter tests

Sample	TTI/s	ΔTTI/%	Avg HRR/kW m^{-2}	pk HRR/kW m^{-2}	Δpk HRR/%	TSR/m^2 m^{-2}	ΔTSR/%
PE	114 ± 4	–	548 ± 12	950 ± 30	–	1,494 ± 52	–
PE-Ar974-2	136 ± 3	+19	524 ± 3	785 ± 2	−17	1,760 ± 175	+18
PE-Ar974-4	129 ± 6	+13	485 ± 12	709 ± 8	−25	1,580 ± 46	+5
PE-Ar974-8	129 ± 6	+13	428 ± 6	609 ± 9	−36	1,747 ± 107	+17
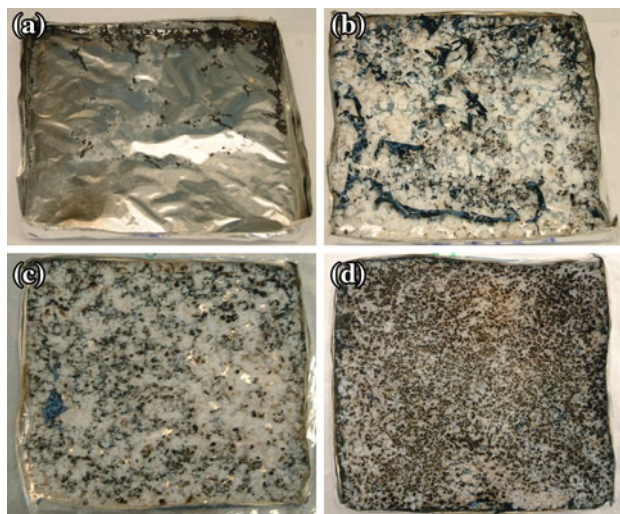
Fig. 9 Cone residues of neat PE and relative nanocomposites. **a** PE, **b** PE-Ar-974-2, **c** PE-Ar-974-4 and **d** PE-Ar-974-8

measuring significant parameters as time to ignition, THR and HRR (and the relative peak) and TSR. The HRR is plotted for each sample in Fig. 8, while Table 4 lists combustion data of PE and relative nanocomposites acquired by the cone calorimetry. In general, a delay of the time to ignition can be observed as a consequence of nanofiller addition, and this is surely a relevant and quite unusual result for nanocomposite materials. In fact, in a recent review of Kiliaris [28] collecting several cone calorimeter data for nanocomposites, most of them reported a decrease of TTI, also for PE-based nanocomposites. Moreover, a reduction of the average HRR and the peak of HRR has been found for all the formulations. This reduction of HRR is proportional to the amount of nanosilica dispersed into the matrix. The presence of silica increases instead the quantity of smoke produced that is one of the important risk factors during fire. As already discussed in the "Flammability test" the mechanism of flame retardancy involved in these materials is a physical barrier of the char layers supported by the presence of the inorganic particles. In Fig. 9, the pictures of sample residues of the various materials after the cone calorimetry test are reported, from which it is clear that the amount of char layer markedly increases with the increases of the silica amount in the samples.

Conclusions

Various amounts of surface-treated fumed silica nanoparticles were melt compounded with a high-density polyethylene matrix, in order to study the thermal resistance and flammability properties of the resulting nanocomposites.

The results of TG analysis highlighted the capability of the selected nanoparticles in increasing the decomposition temperature and in decreasing the mass loss rate, while limiting oxygen values were noticeably improved with respect to the unfilled matrix. Moreover, functionalized nanoparticles revealed extremely effective in delaying the time to ignition and in suppressing HRR values, while the presence of an evident matrix charring for nanofilled sample only slightly increased the quantity of smoke produced. Therefore, the selected nanoparticles revealed particularly efficient in increasing the thermal stability and the combustion resistance of polyethylene matrices even at low filler concentrations.

Finally, it is worthwhile to underline that, due to the homogeneous dispersion of silica aggregates within the matrix, a stiffening effect was detected for nanofilled samples with a substantial preservation of the ultimate tensile properties at break, even at elevated filler amounts.

References

1. Bondioli F, Dorigato A, Fabbri P, Messori M, Pegoretti A. High-density polyethylene reinforced with submicron titania particles. Polym Eng Sci. 2008;48:448–57.
2. Bondioli F, Dorigato A, Fabbri P, Messori M, Pegoretti A. Improving the creep stability of high-density polyethylene with acicular titania nanoparticles. J Appl Polym Sci. 2009;112:1045–55.
3. Mandalia T, Bargaya F. Organo-clay mineral-melted polyolefin nanocomposites. Effect of surfactant/CEC ratio. J Phys Chem Solids. 2005;67:836–45.
4. Yuan Q, Misra RDK. Impact fracture behaviour of clay-reinforced polypropylene nanocomposites. Polymer. 2006;47:4421–33.
5. Zhang Z, Yang JL, Friedrich K. Creep resistant polymeric nanocomposites. Polymer. 2004;45:3481–5.
6. Zhao C, Qin H, Gong F, Feng M, Zhang S, Yang M. Mechanical, thermal and flammability properties of polyethylen/clay nanocomposites. Polym Degrad Stab. 2005;87:183–9.

7. Zhang MQ, Rong MZ, Zhang HB, Friedrich K. Mechanical properties of low nano-silica filled high density polyethylene composites. Polym Eng Sci. 2003;43(2):490–500.

8. Zhang J, Jiang DD, Wilkie CA. Polyethylene and polypropylene nanocomposites based upon an oligomerically modified clay. Thermochim Acta. 2005;430:107–13.

9. Pegoretti A, Dorigato A, Penati A. Tensile mechanical response of polyethylene–clay nanocomposites. Express Pol Lett. 2007;1(3):123–31.

10. Starkova O, Yang JL, Zhang Z. Application of time-stress superposition to nonlinear creep of polyamide 66 filled with nanoparticles of various sizes. Compos Sci Technol. 2007;67:2691.

11. Choi WJ, Kim SH, Kim YJ, Kim SC. Synthesis of chain-extended organifier and properties of polyurethane–clay nanocomposites. Polymer. 2004;45(17):6045–57.

12. Gorrasi M, Tortora M, Vittoria G. Synthesis and physical properties of layered silicates/polyurethane nanocomposites. J Polym Sci B. 2005;43(18):2454–67.

13. Tortora M, Gorrasi M, Vittoria G, Galli V, Ritrovati S, Chiellini E. Structural characterization and transport properties of organically modified montmorillonite/polyurethane nanocomposites. Polymer. 2002;43(23):6147–57.

14. Zhang M, Sundararaj U. Thermal, rheological, and mechanical behaviors of LLDPE/PEMA/clay nanocomposites: effect of interaction between polymer, compatibilizer, and nanofiller. Macromol Mater Eng. 2006;291:697–706.

15. Ou CF, Hsu MC. Preparation and properties of cycloolefin copolymer/silica hybrids. J Appl Polym Sci. 2007;104:2542–8.

16. Ou CF, Hsu MC. Preparation and characterization of cyclo olefin copolymer (COC)/silica nanoparticle composites by solution blending. J Polym Res. 2007;14:373–8.

17. Kolarik J, Fambri L, Pegoretti A, Penati A, Goberti P. Prediction of the creep of heterogeneous polymer blends: rubber-toughened polypropylene/poly(styrene-co-acrylonitrile). Polym Eng Sci. 2002;42(1):161–9.

18. Kolarik J, Pegoretti A, Fambri L, Penati A. Non linear long term tensile creep of polypropylene/cycloolefin copolymer blends with fibrous structure. Macromol Mater Eng. 2003;288:629–41.

19. Pegoretti A. Creep and fatigue behaviour of polymer nanocomposites. In: Karger-Kocsis J, Fakirov S, editors. Nano- and micromechanics of polymer blends and composites. Munich: Carl Hanser Verlag GmbH & Co. KG; 2009. p. 301–39.

20. Bergaya F, Mandalia T, Amigouet P. A brief survey on CLAY-PEN and Nanocomposites based on unmodified PE and organo-pillared clays. Colloid Polym Sci. 2005;283:773–82.

21. Su S, Jiang DD, Wilkie CA. Poly(methyl methacrylate), polypropylene and polyethylene nanocomposite formation by melt blending using novel polymerically modified clay. Polym Degrad Stab. 2004;83:321–31.

22. Wang KH, Xu M, Choi YS, Chung IJ. Effect of aspect ratio on melt extensional process of maleated polyethylene/clay nanocomposites. Polym Bull. 2001;46:499–595.

23. Lu H, Hu Y, Xiao J, Kong Q, Chen Z, Fan W. The influence of irradiation on morphology evolution and flammability properties of maleated polyethylene/clay nanocomposite. Mater Lett. 2005;59:648–51.

24. Ranade A, Nayak K, Fairbrother D, D' Souza NA. Maleated and non maleated polyethylene-montmorillonite layered silicate blown films: creep, dispersion and crystallinity. Polymer. 2005;46:7323–33.

25. Costantino U, Gallipoli A, Nocchetti M, Camino G, Bellucci F, Frache A. New nano-composites constituted of polyethylene and organically modified ZnAl-hydrotalcites. Polym Degrad Stab. 2005;90:586–90.

26. Costantino U, Montanari F, Nocchetti M, Canepa F, Frache A. Preparation and characterization of hydrotalcite/carboxy-adamantane intercalation compounds as fillers of polymeric nanocomposites. J Mater Chem. 2007;17:1079–86.

27. Gilman JW. Flammability and thermal stability studies of polymer layered-silicate (clay) nanocomposites. Appl Clay Sci. 1999;15(1–2):31–49.

28. Kiliaris P, Papaspyrides CD. Polymer/layered silicate (clay) nanocomposites: an overview of flame retardancy. Prog Polym Sci. 2010;35:902–58.

29. Dorigato A, Pegoretti A, Penati A. Linear low-density polyethylene/silica micro- and nanocomposites: dynamic rheological measurements and modelling. Express Pol Lett. 2010;4(2):115–29.

30. Dorigato A, Dzenis Y, Pegoretti A. Nanofiller aggregation as reinforcing mechanism in nanocomposites. Procedia Eng. 2011;10:894-899.

31. Dorigato A, Fambri L, Pegoretti A, Slouf M, Kolarik J. Cyclo-olefin copolymer (COC)/fumed silica nanocomposites. J Appl Polym Sci. 2011;119:3393–402.

32. Dorigato A, Pegoretti A. Tensile creep behaviour of polymethylpentene/silica nanocomposites. Polym Int. 2010;59:719–24.

33. Dorigato A, Pegoretti A, Kolarik J. Nonlinear tensile creep of linear low density polyethylene/fumed silica nanocomposites: time-strain superposition and creep prediction. Polym Compos. 2010;31:1947–55.

34. Kontou E, Niaounakis M. Thermo-mechanical properties of LLDPE/SiO$_2$ nanocomposites. Polymer. 2006;47:1267–80.

35. Barus S, Zanetti M, Lazzari M, Costa L. Preparation of polymeric hybrid nanocomposites based on PE and nanosilica. Polymer. 2009;50:2595–600.

36. Chrissafis K, Paraskevopoulos KM, Pavlidou E, Bikiaris D. Thermal degradation mechanism of HDPE nanocomposites containing fumed silica nanoparticles. Thermochim Acta. 2009;485:65–71.

37. Chrissafis K, Paraskevopoulos KM, Tsiaoussis I, Bikiaris D. Comparative study of the effect of different nanoparticles on the mechanical properties, permeability, and thermal degradation mechanism of HDPE. J Appl Polym Sci. 2009;114:1606–18.

38. Dorigato A, D'Amato M, Pegoretti A. Thermo-mechanical properties of high density polyethylene - fumed silica nanocomposites: effect of filler surface area and treatment. J Polym Res. 2012 (in press).

39. Sinha Ray S, Okamoto M. Polymer/layered silicate nanocomposites: a review from preparation to processing. Prog Polym Sci. 2003;28:1539–641.

40. Vassiliou A, Bikiaris D, Pavlidou E. Optimizing melt-processing conditions for the preparation of iPP/fumed silica nanocomposites: morphology, mechanical and gas permeability properties. Macromol React Eng. 2007;1:488–501.

41. Naveau E, Dominkovics Z, Detrembleur C, Jérôme C, Hári J, Renner K, et al. Effect of clay modification on the structure and mechanical properties of polyamide-6 nanocomposites. Eur Polym J. 2011;47(1):5–15.

42. Pukanszky B, Demjen Z. Silane treatment in polypropylene composites: adsorption and coupling. Macromol Symp. 1999;139:93–105.

43. Ábrányi Á, Százdi L, Pukánszky B, Vancsó GJ. Formation and detection of clay network structure in poly(propylene)/layered silicate nanocomposites. Macromol Rapid Commun. 2006;27(2):132–5.

44. Lertwimolnun W, Vergnes B. Influence of compatibilizer and processing conditions on the dispersion of nanoclay in a polypropylene matrix. Polymer. 2005;46(10):3462–71.

45. Akbari B, Bagheri R. Deformation mechanism of epoxy/clay nanocomposite. Eur Polym J. 2007;43:782–8.

46. Shen L, Du Q, Wang H, Zhong W, Yang Y. In situ polymerization and characterization of polyamide-6/silica nanocomposites derived from water glass. Polym Int. 2004;53:1153–60.

47. Gungor A. The physical and mechanical properties of polymer composites filled with Fe powder. J Appl Polym Sci. 2006;99: 2438–42.

48. Pan M, Shi X, Li X, Hu H, Zhang L. Morphology and properties of PVC/Clay nanocomposites via in situ emulsion polymerization. J Appl Polym Sci. 2004;94:277–86.

49. Bikiaris DN, Vassiliou A, Pavlidou E, Karayannidis GP. Compatibilisation effect of PP-*g*-MA copolymer on iPP/SiO$_2$ nanocomposites prepared by melt mixing. Eur Polym J. 2005;41: 1965–78.

50. Costa FR, Wagenknecht U, Heinrich G. LDPE/Mg–Al layered double hydroxide nanocomposite: thermal and flammability properties. Polym Degrad Stab. 2007;92:1813–23.

51. Garcia N, Hoyos M, Guzman J, Tiemblo P. Comparing the effect of nanofillers as thermal stabilizers in low density polyethylene. Polym Degrad Stab. 2009;94:39–48.

52. Leszczynska A, Njuguna J, Pielichowski K, Banerjee JR. Polymer/montmorillonite nanocomposites with improved thermal properties. Part I. Factors influencing thermal stability and mechanisms of thermal stability improvement. Thermochim Acta. 2007;453:75–96.

53. Stark NM, White RH, Mueller SA, Osswald TA. Evaluation of various fire retardants for use in wood flourepolyethylene composites. Polym Degrad Stab. 2010;95:1903–10.

54. Minkova L, Peneva Y, Tashev E, Filippi S, Pracella M, Magagnini P. Thermal properties and microhardness of HDPE/clay nanocomposites compatibilized by different functionalized polyethylenes. Polym Test. 2009;28:528–33.

55. Elias HG. An introduction to plastics. Weinheim: Wiley-VCH; 2003.

56. Cassagnau P. Melt rheology of organoclay and fumed silica nanocomposites. Polymer. 2008;49:2183–96.